Proceedings World Geothermal Congress 2023
Beijing, China, April 17 – 21, 2023

# Experimental study of the heat transfer characteristics of single geothermal fracture

Biao Shu, Runjun Zhu, Jingqiang Tan

School of Geosciences and Info-Physics, Central South University, Changsha, Hunan, P. R. China 410083

biaoshu@csu.edu.cn

**Keywords:** Geothermal energy, Permeability, Heat transfer, Confining pressure, Hydraulic aperture

## ABSTRACT

Mineral dissolution and mechanical deformation of granite are two main mechanisms that affect permeability evolution of rock fracture. In this study, two water flow-through experiments with large granite fractures were conducted at 200 ℃ with a constant flow rate for 24 h, under confining pressures of 5 and 10 MPa, respectively. Water pressure and temperature were measured, fracture aperture and permeability were calculated, and chemical element concentrations in effluent water were tested for mechanism analysis. The permeability fluctuates up and down between 2.62×10-12 and 3.16×10-12 m2 at confining pressure of 5 MPa; while it decreased monotonously by 24% from 1.92×10-12 to 1.45×10-12 m2 at a confining pressure of 10 MPa. The heat transfer rates at both experiments stay stable at about 0.25 J/s. The mass concentration of Ca, Na, K, and Si in effluent water are between 5 to 23 mg/L, indicating slight dissolution of Ca-plagioclase, Na-plagioclase, and K-feldspar, as well as possible precipitation of minor amount of Kaolinite or Qartz. The total amount of free-face dissolution and pressure dissolution are similar at 5 and 10 MPa. The geochemical reaction counts only small part of aperture change, and the mechanical deformation counts the major part of aperture change.

## 1. INTRODUCTION

Geothermal energy is a type of promising low carbon energy that can reduce fossil energy consumption and carbon dioxide emissions (Regenauer-Lieb et al., 2015; Ma et al., 2019). The total installed power plant capacity of geothermal was 14.9 GW worldwide in 2019 (Richter, 2019), and it is estimated to reach up to 140 GW by 2050 (Bertani, 2016). One percent of the total estimated geothermal energy in the world can provide 2500 years of power (Olasolo, 2016).

The enhanced geothermal system (EGS) is considered the most feasible and commonly accepted method to develop baseload scale geothermal energy from hot dry rocks (HDR) (Bentz et al., 2020). In EGSs, drilling and stimulation are first used to enhance the permeability of geothermal reservoir (Frash et al., 2014), and then, the working fluid (such as water) is injected into geothermal reservoir rocks through an injection well and then pumped to the ground surface through an outlet well after extracting heat from hot rocks (Olasolo et al., 2016). For a successful geothermal energy production of EGS, a high density of artificial fractures created by hydraulic fracturing is required to provide conductive flow pathways, as well as a sufficient contact area between the heat transfer medium, such as water, and the hot dry rocks (Wu et al., 2016; Guo et al., 2019; Shu et al., 2019a). The heat extraction and the temperature of water flowing through fractures in EGS can be calculated with a semi-analytical solution (Wu et al., 2015, 2017). Fluid movement in fracture networks is of critical importance to geothermal energy extraction (Bai et al., 2017).

The permeability of fracture networks is a highly important factor that affects the heat production efficiency and longevity of EGSs (Yasuhara et al., 2006; Zhong et al., 2016; Parisio et and Yoshioka, 2020). Permeability reduction with increased duration of circulation (Morrow et al., 2001) and/or increased confining pressure (Yasuhara et al., 2004) has been reported. Additionally, fracture permeability evolution is more sensitive to temperature and confining pressure compared with the permeability of porous media (Moore et al., 1994; Durham et al., 2001; Polak et al., 2003).

Geochemical dissolution (i.e., pressure dissolution and free-face dissolution) and stress mechanical deformation are two main factors affecting fracture permeability (Yasuhara et al., 2004; Moore et al., 1994; Durham et al., 2001). It was discovered that dissolution and precipitation of minerals occurred at the granitic rock fracture surface during a flow through experiment (Qiao et al., 2019). Among these factors, free-face dissolution can increase the permeability because the mineral mass is net removed from the fracture surface (Liu et al., 2006; Taron and Elsworth, 2009); however, the pressure dissolution of fracture propping asperities can cause permeability decrease (Polak et al., 2004). Mineral precipitation on fracture surface, resulting from mineral dissolution, may slightly change the fracture permeability (Yasuhara et al., 2011). Dissolution and precipitation of minerals at hydrothermal conditions have been observed using scanning electron microscopy and inductively coupled plasma analysis (Morrow et al., 2001). Some minerals are easier to be dissolved in water, such as calcite, feldspar, and biotite, whereas other minerals are much more difficult to be dissolved, such as quartz (Savage et al., 1992). In addition to mineral dissolution, mechanical processes at contacting asperities of a fracture surface may be another important factor causing fracture aperture and permeability change at confining pressures (Yasuhara et al., 2011). A previous study has shown that rock material compressibility and fracture deformation during thermal-hydro coupling processes can significantly affect the discontinuity conductivity of geothermal reservoirs (Chen et al., 2020).

Experimental studies regarding the permeability evolution pertaining to THMC coupling have been reported; however, most of those studies were conducted on non-granite rocks, such as novaculite (Polak et al., 2003) or limestone (Polak et al., 2004); only a few experimental studies have been performed in granite-rock-type EGS reservoirs (Caulk et al., 2016). In these experimental studies of fracture permeability, most of the experiments were conducted at temperatures less than 150 ℃ or on small rock specimens less than 50 mm long. The main mechanism of chemical dissolution and stress deformation of granite may differ when different compressive pressures were applied on the fracture surface. In conclusion, long-term fluid flow-through experimental

studies based on real EGS temperatures and large granite fractures are lacking for investigating the THMC mechanism of the permeability evolution under different in situ stresses. The reservoir pressure and temperature variation are the most important factors affecting the water-rock reaction (Zheng et al., 2019). Therefore, in this paper, water flow-through experiments of granite fractures were conducted to explore the effect of in situ stress on fracture permeability under high temperature, and the chemical and mechanical processes behind.

Two flow-through experiments were conducted on a novel experiment device at 200 ℃ for 24 h under confining pressures of 5 and 10 MPa. Granite rock samples were collected from a major deep geothermal reservoir area, and the temperature used resembled the actual EGS temperature. The pressure and temperature of influent and effluent water were collected continuously to calculate the hydraulic aperture, permeability, and heat transfer rate. It was discovered that the permeability evolution differed vastly owing to the different confining pressures. Chemical element concentrations were tested with effluent water samples. Based on the results, the mechanism of mineral dissolution and mechanical deformation were analyzed and discussed. It was discovered that the permeability evolution in the EGS reservoir environment depended significantly on the confining pressure, but the heat transfer rate was not affected. The result of this study can provide insight into the effects of in situ stresses on the hydraulic properties and heat recovery properties of EGS reservoirs; therefore, it is crucial to the evaluation of geothermal energy production efficiency.

## 2. MATERIALS AND METHODS

Geothermal energy is usually preserved in granite rocks (Xiao et al., 2020), so flow-through experiments were performed on two granite rock samples. The mineral contents of the rock sample, obtained by X-ray diffraction (XRD) analysis, are composed of 25% of quartz, 45% K-feldspar, 25% plagioclase, and 5% biotite. The mineral grain size was between 0.5 and 2.0 mm. The density of the granite samples was 2.65 g/cm3.

Each cylinder granite core, measuring 50 mm in diameter and 100 mm in length, was split into two halves make it an artificial rough fracture, as shown in Fig. 1 (a). The two semi-cylinders of each sample were placed together and fit closely in the same manner as before they were split. Polymer tape and soft copper sleeve were used to prevent water leakage and maintain confining pressure.

The experimental device, as shown in Fig. 1 (b), can conduct high temperature high pressure fluid flow-through test, with maximum temperature of 350 ℃ and maximum pressure of 50 MPa. It primarily includes a heatable core holder, confining pressure pump, and pore pressure pump, pressure sensors, and temperature sensors. The core holder can heat rock sample to predetermined temperature. The confining pressure, fluid pressure, rock temperature, and flow rate were controlled and monitored using a computer. More details regarding the experimental device is shown in Fig. 2, and its mechanism are reported in a previous study (Shu et al., 2019b). This new study steps forward on the basis of our previous studies, and focused on the effect of in situ stress on the permeability change, and the mechanism behind that.


**Figure 1. (a) One split granite rock sample and (b) Fluid flow-through experiment device.**

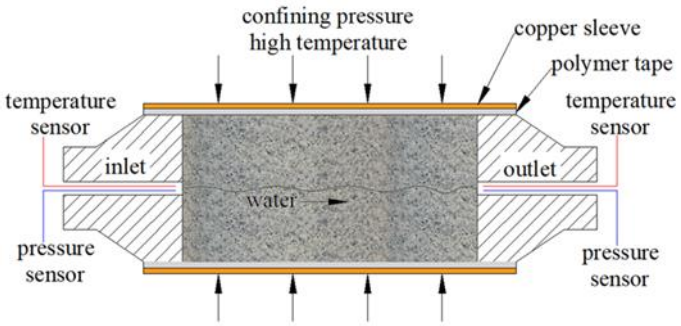


**Figure 2. Schedule of water flow-through experiment (not to scale).**

Two water flow-through experiments were conducted at 200 ℃, under confining pressures of 5 and 10 MPa, separately. Each flow-through process lasted 1440 min (24 h), and the flow rate was maintained at 1.0 ml/min at all times. The experimental parameters are shown in Table 1.

**Table 1 Experimental parameter design.**

| Experiment | Confining pressure, MPa | Temperature, ℃ | Flow rate, ml/min | Flow time, min |
|---|---|---|---|---|
| #1 | 5 | 200 | 1.0 | 1440 |
| #2 | 10 | 200 | 1.0 | 1440 |

The experiment can be described as below:

(1) Install fracture sample into the coreholder, gradually increase the temperature of sample to 200 ℃ at a rate of 5 ℃/h, and the temperature was hold for 2 hours which is sufficient for thermal equilibration (Browing et al., 2016);

(2) The confining pressure was increased to 5 or 10 MPa;

(3) Water was injected into the fracture and the flow rate was maintained at 1.0 ml/min;

(4) After the water flow reached a steady state in the fracture, the water temperatures and water pressures at both the outlet and inlet were recorded continuously for 1440 min.

## 3. RESULTS

The water pressures at both sides of fractures were recorded in the experiments. The water pressure of outlet was set to be larger than 1.62 MPa to retain water at the liquid state (Shu et al., 2019b; Shu et al., 2020). The water pressure drop from the inlet to the outlet was the pressure required for the fluid to flow through the fracture. The water pressure differences are plotted in Fig. 3.

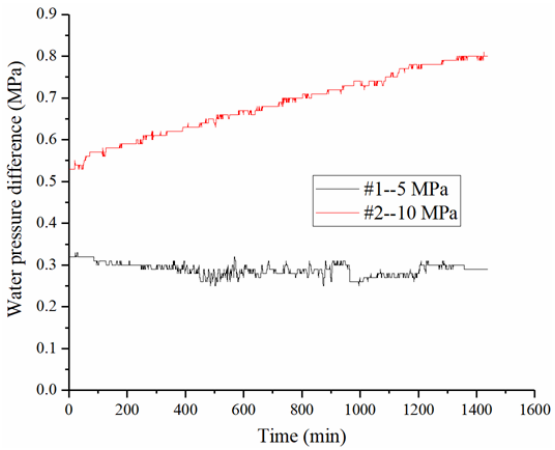


**Figure 3. Fluid pressure differences between inlet and outlet at flow-through experiments.**

As shown in Figure 3, the water pressure difference, at a confining pressure of 5 MPa, generally stayed at about 0.3 MPa and only fluctuated slightly. However, the water pressure difference at the confining pressure of 10 MPa persistently increased from 0.53 to 0.80 MPa. Overall, the water pressure difference at confining pressure of 10 MPa is about two times of that at confining pressure of 5 MPa. Hence, more power was required to transport the same amount of water to flow through the reservoir fractures in higher in situ stress conditions, and the power will increase with increased circulation duration.

The density, specific heat capacity and dynamic viscosity applicable to the following calculation of heat transfer and hydraulic properties can be inferred from Fig. 4 (Shu et al., 2022), which was calculated based on equaitons described by Qu et al. (2017). As shown in this figure, as the temperature increased, the water dynamic viscosity and density decreased. The specific heat capacity first decreased and then increased as the temperature increased.

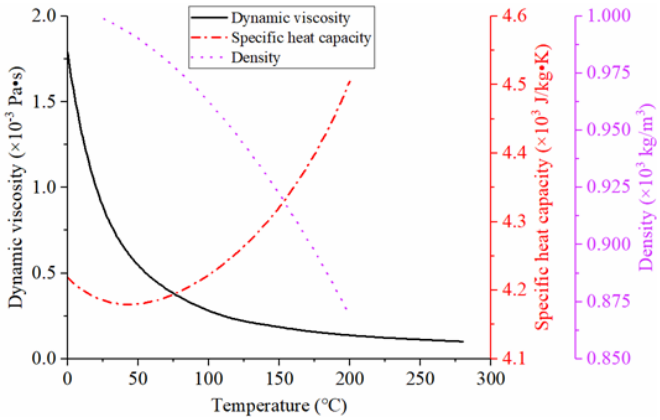


**Figure 4. Changes of density, specific heat capacity, and dynamic viscosity of water with temperature (modified from Shu et al. (2022)).**

It has been proved by many experimental studies that Darcy's law and cubic law are valid for water flow in deformable rock fracture (Iwai, 1976; Witherspoon et al., 1980). Many more recent studies (Morrow et al., 2001; Polak et al., 2003; Liu et al., 2006; Caulk et al., 2016; Ma et al., 2019; Klepikova, 2021), also consider Darcy's law and cubic law can be directly used for fluid flow-through experimental and numerical modeling at different confining stresses and temperatures. Therefore, we used Darcy's law and cubic law in our data analysis.

The modified cubic law, representing water flow through a single granite fracture, was shown in Equation (1) (Witherspoon et al., 1980).

$$q = \frac{Pdb_e^{\,3}}{12\mu L} \tag{1}$$

where $q$ is flow rate (m3/s), $P$ is pressure drop from inlet to outlet (Pa), $d$ is fracture width (sample diameter) (m), $b_e$ is equivalent hydraulic aperture (m), $\mu$ is water dynamic viscosity (Pa s), and $L$ is flow distance (fracture length) (m).

Transforming Eq. (1), the be can be represented as

$$b_e = \sqrt[3]{\frac{12q\mu L}{Pd}} \tag{2}$$

The calculated hydraulic aperture changes in these two experiments are shown in Fig. 5. The initial hydraulic aperture of experiment #1 is larger than that of experiment #2. This is because the higher confining pressure enables the fracture to be more tightly closed. As the flow time progressed, the hydraulic fracture of experiment #1 fluctuated severely but remained in a small range. Overall, it first increased gradually from 5.7 ×10-6 m to approximately 6.0 ×10-6 m and then decreased to 5.9 ×10-6 m. In experiment #2, it is clear that the hydraulic aperture decreased stably from approximately 4.8 ×10-6 to 4.2 ×10-6 m. In a previous study, under the confining pressure of 20 MPa, the hydraulic aperture decreased by 14.3% in 1440 min (Shu et al., 2019b), while in our current study at the confining pressure of 10 MPa, the hydraulic aperture decreased by 12.5%, which means the higher the confining pressure, the faster the hydraulic aperture decreases.

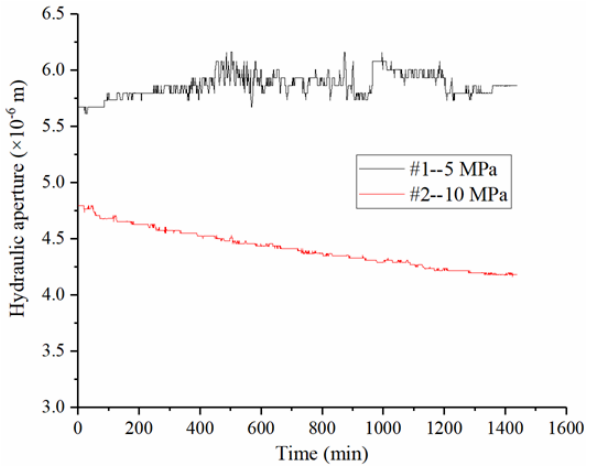


**Figure 5. Hydraulic apertures in flow-through experiments.**

The permeability of a single fracture can be described by Darcy's law (Caulk et al., 2016).

$$k_e = \frac{q \cdot \mu \cdot L}{P \cdot A} \tag{3}$$

where $k_e$ is the permeability of the fracture ($m^2$), and $A$ is the cross sectional area of the fracture ($m^2$) expressed as

$$A = d \cdot b_e \tag{4}$$

Hence, the permeability $k_e$ can also be calculated by combining Equations (2), (3), and (4), as follows

$$k_e = \frac{{b_e}^2}{12} = \frac{1}{12} \cdot \left(\frac{12q\mu L}{Pd}\right)^{2/3} \tag{5}$$

The permeability changes of these two experiments are shown in Fig. 6. The change trends of permeability were the same as those of the hydraulic aperture. At the confining pressure of 5 MPa, the permeability changed slightly in the entire experiment but fluctuated severely. At the confining pressure of 10 MPa, the permeability decreased monotonously by 24%. In a previous study, permeability decreased by 27% under a confining pressure of 20 MPa at the same temperature of 200 ℃ for a same duration of 1440 min (Shu et al., 2019b). From the experimental results, we may predict that the permeability decreases more significantly under higher confining pressure.

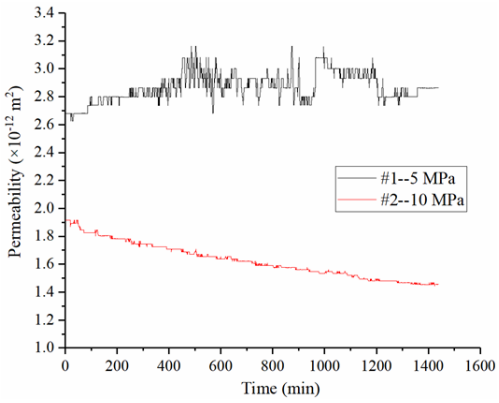


**Figure 6. Permeability changes in flow-through experiments.**

The heat transferred from the fracture to water was calculated as follows

$$Q = q\rho c(T_o - T_i) \tag{6}$$

where $Q$ is the heat transfer rate (J/s), $T_o$ is the effluent water temperature (K), and $T_i$ is the influent water temperature (K).

The influent water was warmed up to certain high temperature before it enters the rock fracture, so in fact, during the experiment, the temperature of influent water is not as low as we thought. In these two experiments, the influent water temperatures were both around 186.9-187.2 ℃, and the effluent water temperatures were both around 190.6-191.0 ℃. The temperature difference between influent water and rock fracture is not very large, therefore, it is not going to have a large effect on the rock deformation and fracture aperture. As we can see from Fig. 8 (a) and (b), during the whole tests, the fluctuation of influent and effluent water temperatures are very minor and can be ignore.

The heat transfer rate is only related to flow rate, water density, water heat specific capacity, and water temperature increasement. In these two experiments, all these parameters were almost the same and hence the heat transfer rates. As shown in Fig. 7 (c) and (d), the heat transfer rates are both stay stable at about 0.25 J/s.

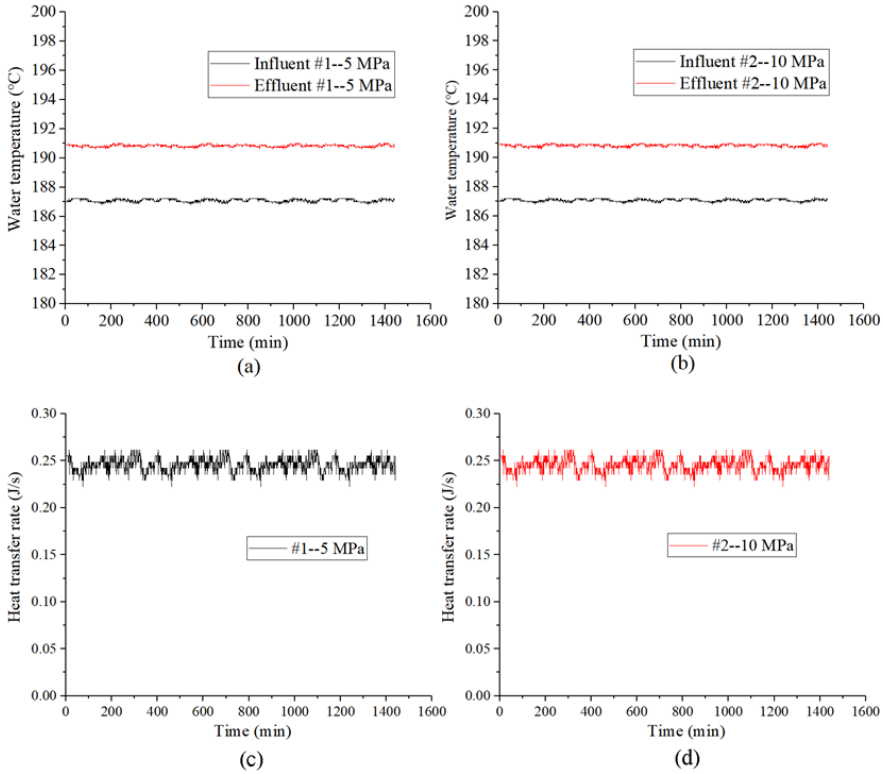


**Figure 7. (a) Water temperatures of experiment #1; (b) water temperatures of experiment #2; (c) heat transfer rate of experiment #1; (d) heat transfer rate of experiment #2.**

This indicated that regardless of the change in the hydraulic aperture and permeability, the water temperature increased from the inlet to the outlet remained unchanged. This could be because the flow rate was small, and regardless of whether it was flowing slightly faster or slower, the water could be fully heated, provided that the rock sample temperatures were the same.

In this study, plasma emission spectrometry was performed to examine the mass concentration elements in the effluent water. The average mass concentrations obtained from the effluent water of experiments #1 and #2 are listed in Table 2. The mass concentrations of Ca, Na, K, and Si in experiment #1 were 16.33, 13.32, 7.28, and 22.44 mg/L, respectively, whereas those of Ca, Na, K, and Si in experiment #2 were 16.42, 12.43, 5.90, and 13.97 mg/L, respectively. The mass concentrations of Al and Mg were less than 0.3 mg/L in both experiments.

**Table 2 Average mass concentrations of chemical element in effluent water**

| Element | Average mass concentration at experiment #1, mg/L | Average mass concentration at experiment #2, mg/L |
|---|---|---|
| Ca | 16.33 | 16.42 |
| Na | 13.32 | 12.43 |
| K | 7.28 | 5.90 |
| Si | 22.44 | 13.97 |
| Al | < 0.3 | < 0.3 |
| Mg | < 0.3 | < 0.3 |

## 4. ANASYSIS AND DISCUSSION

### 4.1 Chemical Analysis

Previous studies have disclosed that many chemical elements were dissolved in the EGS fluid pumped out of an outlet well (Savage et al., 1992). Therefore, it is crucial to perform a chemical analysis in the flow-through experiments. Caulk et al. (2016) collected influent and effluent water from granite fracture flow through tests; subsequently, they acidified water and analyzed for Si, Al, Ca, Mg, K, Na, and Fe by elemental analysis. They discovered that the dissolution of K, Ca, and Na implied the dissolution of K-feldspar and plagioclase, as well as the precipitation of kaolinite.

Savage et al. (1992) reported that quartz was difficult to be dissolved; therefore, we may ignore quartz dissolution in this study also. In the following analysis, we can primarily focus on the dissolution of Ca-plagioclase, Na-plagioclase, and feldspar.

However, it is also not easy to find out which mineral was generated and precipitated at fracture surface. Because the amount of precipitation is too little, it was unable to tell which mineral it was even with particle-induced X-ray emission (PIXE) analysis, and it was only able to find the presence of Si in the precipitation (Caulk et al., 2016). Caulk et al. (2016) believed that the low ratios of Si to Ca, Na, and K was owing to the formation of kaolinite (Al2Si2O5(OH)4), which consumed a large amount of Si. This may also explain the low concentration of Al in the effluent water.

In our experiments, a very thin film of white mineral was observed on the fracture surfaces after the flow-through experiments. However, the mineral precipitation at our test is even less than that in Caulk et al (2016)'s experiments, so it is impossible to collect them for PIXE analysis. In conclusion, some form of mineral must be formed and precipitated at the fracture surface. It may be kaolinite, or other minerals, such as quartz.

Geochemical dissolution primarily involves pressure dissolution (Polak et al., 2004) occurring at contact asperities, and free-face dissolution (Liu et al., 2006) at free-fracture surfaces. Owing to the different confining pressure, more contacting asperities exist at the fracture surface of higher confining pressure. It resulted in stronger pressure dissolution and less free-face dissolution in experiment #1. On contrary, more extensive free-face dissolution and less pressure dissolution occurred in experiment #2. The total amounts of pressure dissolution plus free-face dissolution in both experiments are quite small and their effect to hydraulic aperture is very minor.

### 4.2 Mechanical Analysis

As we mentioned in Fig. 5, the fracture aperture of experiment #1 only slightly fluctuate but did not change very much, but it decreases consistently in experiment #2. Previous study found fracture aperture always decreases with increased duration of circulation (Caulk et al., 2016), but in experiment #1, the fracture aperture obviously did not decrease. In these two experiments, the total dissolutions were at the same level, whereas the precipitation only affected the fracture aperture or permeability slightly (Yasuhara et al., 2011), but the fact is that there is significant difference in the fracture aperture change between these two experiments. Therefore, geochemical reaction should only count a small part of the fracture aperture change, and the main mechanism should be the mechanical deformation (Caulk et al., 2016).

At the confining pressure of 5 MPa, the contact stress on the fracture surface is small; as such, the pressure dissolution was not strong and the mechanical deformation of contact asperities was small. Therefore, the fracture aperture did not decrease. In addition, owing to the low effective normal pressure, the fracture was not stably closed when water was flowing in the fracture; hence, the aperture may fluctuate severely.

On the contrary, at the confining pressure of 10 MPa, the contact stress on the fracture surface is high; therefore, more pressure dissolution and mechanical deformation occurred on the contact asperities, which decreased the aperture. Additionally, owing to the high normal pressure, the fracture was more stably closed; therefore, the fracture aperture did not fluctuate significantly.

The permeability change mechanism, i.e., geochemical dissolution and mechanical deformation, can be summarized as follows:

(1) Pressure dissolution, mineral precipitation, and mechanical deformation decreased the permeability, whereas free-face dissolution increased the permeability.

(2) For low confining pressures (such as 5 MPa), less pressure dissolution, more extensive free-face dissolution, less precipitation, and slight mechanical deformation occurred. Overall, the fracture permeability did not change significantly.

(3) For high confining pressures (such as 10 MPa), more pressure dissolution, less free-face dissolution, more precipitation, and strong mechanical deformation occurred. Overall, the fracture aperture and permeability decreased steadily.

## 5. CONCLUSIONS

This study focused on the analysis of the permeability and heat transfer evolution. Two long-term flow-through experiments were conducted at 200 ℃ and a constant flow rate of 1.0 ml/min, under confining pressures of 5 and 10 MPa respectively. It was discovered that the permeability evolution in the EGS reservoir environment depended significantly on the in situ stress. The result of this study could provide insight into the effects of in situ stresses on the hydraulic properties and heat recovery properties of EGS reservoirs. The conclusions of this study can be summarized as follows:

(1) The hydraulic permeability fluctuated up and down severely between 2.62 ×10-12 and 3.16 ×10-12 m2 at a low confining pressure (5 MPa); however, it decreased monotonously by 24% from 1.92 ×10-12 to 1.45 ×10-12 m2 at a high confining pressure (10 MPa). It is the effective stress acting on the fracture surface determines the fracture aperture/permeability change. A very low effective stress may unable to cause a decrease on the fracture aperture/permeability.

(2) The heat transfer rates at both experiments stay stable at about 0.25 J/s, but the pressure drop at confining pressure is about two times of that at confining pressure of 5 MPa. It indicates that more energy is required to extract the same amount of heat from the higher in situ stress geothermal sites.

(3) The chemistry analysis of the effluent water to determine the mass concentrations of Ca, K, Na, and Si revealed that the dissolution of Ca-plagioclase, Na-plagioclase, and K-feldspar at both experiments. The geochemical reaction, including dissolution and precipitation, are both quite mild, so even with the state of the art test technologies, it is still unable to quantify the geochemical reactions.

(4) The geochemical reaction only contributes very little to the fracture aperture change. The mechanical deformation is most likely the main factor that caused fracture aperture and permeability change.

Shu, Zhu, and Tang.

**REFERENCES**


Bai, B., He, Y. Y., Li, X. C., et al. (2017). Experimental and analytical study of the overall heat transfer coefficient of water flowing through a single fracture in a granite core. Applied Thermal Engineering, 116: 79–90.

Bertani, R. (2016). Geothermal power generation in the world 2010–2014 update report. Geothermics, 60: 31–43.

Bentz, S., Kwiatek, G., Martínez-Garzón, P., et al. (2020). Seismic moment evolution during hydraulic stimulations. Geophysical Research Letters, 47: e2019GL086185.

Browning, J., Meredith, P. G., Gudmundsson, A. (2016). Cooling-dominated cracking in thermally stressed volcanic rocks. Geophysical Research Letters, 43: 8417–8425.

Caulk, R. A., Ghazanfari, E., Perdrial, J. N., et al. (2016). Experimental investigation of fracture aperture and permeability change within Enhanced Geothermal Systems. Geothermics, 62: 12–21.

Chen, Y., Ma, G. W., Wang, H. D., et al. (2020). Optimizing heat mining strategies in a fractured geothermal reservoir considering fracture deformation effects. Renewable Energy, 148: 326–337.

Durham, W. B., Bourcier, W. L., Burton, E. A. (2001). Direct observation of reactive flow in a single fracture. Water Resources Research, 37: 1–12.

Frash, L. P., Gutierrez, M., Hampton, J. (2014). True-triaxial apparatus for simulation of hydraulically fractured multi-borehole hot dry rock reservoirs. International Journal of Rock Mechanics and Mining Sciences, 70: 496–506.

Guo, T. K., Gong, F. C., Wang, X. Z., et al. (2019). Performance of enhanced geothermal system (EGS) in fractured geothermal reservoirs with CO2 as working fluid. Applied Thermal Engineering, 152: 215-230.

Iwai, K. (1976). Fundamental studies of fluid flow through a single fracture: [Dissertation]. University of California, Berkeley. 208.

Klepikova, M., Meheust, Y., Roques C., et al. (2021). Heat transport by flow through rough rock fractures: a numerical investigation. Advances in Water Resources, 156: 104042.

Liu, J. S., Sheng, J. C., Polak, A., et al. (2006). A fully-coupled hydrological-mechanical-chemical model for fracture sealing and preferential opening. International Journal of Rock Mechanics & Mining Sciences, 43: 23–36.

Ma, Y.Q., Zhang, Y.J., Huang, Y.B., et al. (2019). Experimental study on flow and heat transfer characteristics of water flowing through a rock fracture induced by hydraulic fracturing for an enhanced geothermal system. Applied Thermal Engineering, 154: 433–441.

Moore, D. E., Lockner, D.A., Byerlee, J. D. (1994). Reduction of permeability in granite at elevated temperatures. Science, 265: 1558–1561.

Morrow, C. A., Moore, D. E., Lockner, D. A. (2001). Permeability reduction in granite under hydrothermal conditions. Journal of Geophysical Research Solid Earth, 106(B12): 30551–60.

Olasolo, P., Juárez, M. C., Morales, M. P., et al. (2016). Enhanced geothermal systems (EGS): a review. Renewable and Sustainable Energy Reviews, 56: 133–144.

Parisio, F., Yoshioka, K. (2020). Modeling fluid reinjection into an enhanced geothermal system. Geophysical Research Letters, 47: e2020GL089886.

Polak, A., Elsworth, D., Yasuhara, H., et al. (2003). Permeability reduction of a natural fracture under net dissolution by hydrothermal fluids. Geophysical Research Letters, 30(20): 2020.

Polak, A., Elsworth, D., Liu, J. S., et al., 2004. Spontaneous switching of permeability changes in a limestone fracture with net dissolution. Water Resources Research, 40: W035502.

Qiao, L. P. , Huang, A. D., Wang, Z. C., et al. (2019). Alteration of minerals and temporal evolution of solution in reactive flow through granitic rock fractures. International Journal of Rock Mechanics & Mining Sciences, 123: 104105.

Qu, Z. Q., Zhang, W., Guo, T. K. (2017). Influence of different fracture morphology on heat mining performance of enhanced geothermal systems based on COMSOL. International Journal of Hydrogen Energy, 42(29): 18263–18278.

Regenauer-Lieb, K., Bunger, A., Chua, H. T., et al. (2015). Deep geothermal: The 'Moon Landing' mission in the unconventional energy and minerals space. Journal of Earth Science, 26(1): 2–10.

Richter, A. (2019). Global geothermal capacity reaches 14,900 MW – new Top 10 ranking of geothermal countries. https://www.thinkgeoenergy.com/global-geothermal-capacity-reaches-14900-mw-new-top10-ranking/.

Savage, D., Bateman, K., Richards, H. (1992). Granite-water interactions in a flow-through experimental system with applications to the Hot Dry Rock geothermal system at Rosemanowes, Cornwall, U.K. Applied Geochemistry, 7: 223–241.

Shu, B., Zhu, R. J., Zhang, S. H., et al. (2019a). A quantitative prediction method of new crack-initiation direction during hydraulic fracturing of pre-cracks based on hyperbolic failure envelope. Applied Energy, 248: 185–195.

Shu, B., Zhu, R. J., Tan, J. Q., et al. (2019b). Evolution of permeability in a single granite fracture at high temperature. Fuel, 242: 12–22.

Shu, B., Zhu, R. J., Elsworth, D., et al. (2020). Effect of temperature and confining pressure on the evolution of hydraulic and heat transfer properties of geothermal fracture in granite. Applied Energy, 272: 115290.

Shu, B., Wang, Y. M., Zhu, R. J., et al. (2022). Experimental study of the heat transfer characteristics of single geothermal fracture at different reservoir temperature and in situ stress conditions. Applied Thermal Engineering, 207:118195.

Taron, J., Elsworth, D. (2009). Thermal-hydrologic-mechanical-chemical processes in the evolution of engineered geothermal reservoirs. International Journal of Rock Mechanics & Mining Sciences, 46: 855–864.

Witherspoon, P. A., Wang, J. S. Y., Iwai, K., et al. (1980). Validity of cubic law for fluid flow in a deformable rock fracture. Water Resources Research, 16(6): 1016–1024.

Wu, B. S., Zhang, X., Jeffrey, G. R., et al. (2015). Perturbation analysis for predicting the temperatures of water flowing through multiple parallel fractures in a rock mass. International Journal of Rock Mechanics and Mining Sciences, 76: 162-173.

Wu, B. S., Zhang, X., Jeffrey, R. G., et al. (2016). A simplified model for heat extraction by circulating fluid through a closed-loop multiple-fracture enhanced geothermal system. Applied Energy, 183: 1664–1681.

Wu, B. S., Zhang, G. Q., Zhang, X., et al. (2017). Semi-analytical model for an enhanced geothermal system considering the effect of the areal flow between dipole wells on heat extraction. Energy, 138: 290-305.

Xiao, Z. C., Wang, S., Qi, S. H., et al. (2020). Petrogenesis, Tectonic Evolution and Geothermal Implications of Mesozoic Granites in the Huangshadong Geothermal Field, South China. Journal of Earth Science, 31(1): 141–158.

Yasuhara, H., Elsworth, D., Polak, A. (2004). Evolution of permeability in a natural fracture: significant role of pressure solution. Journal of Geophysical Research Solid Earth, 109: B03204.

Yasuhara, H., Kinoshita, N., Ohfuji, H., et al. (2011). Temporal alteration of fracture permeability in granite under hydrothermal conditions and its interpretation by coupled chemo-mechanical model. Applied Geochemistry, 26(12): 2074–2088.

Yasuhara, H., Polak, A., Mitani, Y., et al. (2006). Evolution of fracture permeability through fluid–rock reaction under hydrothermal conditions. Earth and Planetary Science Letters, 244(1): 186–200.

Zheng, X. H., Duan, C. Y., Xia, B. R., et al. (2019). Hydrogeochemical Modeling of the Shallow Thermal Water Evolution in Yangbajing Geothermal Field, Tibet. Journal of Earth Science, 30(4): 870–878.

Zhong, Z., Elsworth, D., Hu, Y. J. (2016). Evolution of strength and permeability in stressed fractures with fluid-rock interactions. Pure and Applied Geophysics, 173: 525–536.